Simulation of Light Diffraction

Zhaofeng Peng

Original version dated Apr. 27, 2023

Translated by ChatGPT on Dec. 12, 2025

Introduction

The purpose of this experiment is to investigate the phenomenon of light diffraction. When a beam of light with wavelength λ illuminates an aperture of characteristic size ρ, diffraction occurs. This diffraction effect generally depends on factors such as the aperture size ρ, the light intensity, and the distances between the light source and the diffracting element as well as between the diffracting element and the observation screen. In the experiment, we use apertures whose sizes satisfy $\lambda < \rho < 10^3\lambda$, such as single slits, multiple slits, circular apertures, and square apertures, as diffraction elements. Under these conditions, the diffraction effects become significant. On the optical table, the light source (He–Ne laser, $\lambda = 6328\,\text{Å}$), the diffracting elements, and the observation screen are assembled into an experimental optical path. When the distance z between the diffracting element and the observation screen is sufficiently large (satisfying $z \gg \rho^2/\lambda$), the resulting light diffraction is Fraunhofer diffraction. The schematic diagram of the experimental apparatus is shown in Fig. 1.

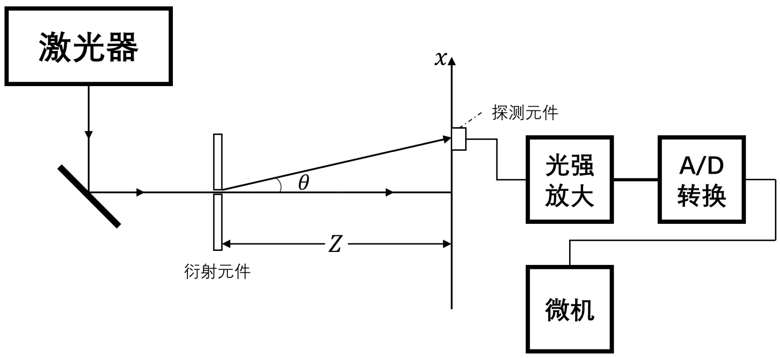

Figure 1: Schematic diagram of the experimental apparatus for quantitative diffraction study

To obtain the diffraction intensity distribution on the screen, we can perform explicit calculation using the complex integral method. This method can be implemented numerically via the fast Fourier transform (FFT) algorithm on a computer. By comparing the diffraction patterns obtained through MATLAB simulation with those observed experimentally, we find that the agreement between the simulation and the actual results is remarkably good.

Theory and Results

Simulation of Fraunhofer diffraction using the fast Fourier transform algorithm.

Using the complex integral method, the intensity distribution formula on the receiving screen can be obtained. The Fresnel–Kirchhoff diffraction integral formula is

$$\widetilde{U}(P) = \frac{-\mathrm{i}}{\lambda} \iint\limits_{\Sigma_0} \widetilde{U}_0(Q) \frac{\mathrm{e}^{\mathrm{i}kr}}{r} f(\theta_0, \theta)\, \mathrm{d}\Sigma$$

where $f(\theta_0, \theta)$ is the inclination factor. Since $f(\theta_0, \theta)$ varies slowly with θ, we may take $f(\theta_0, \theta) = 1$; $\widetilde{U}_0(Q)$ is the complex amplitude of vibration at the slit. Because the incident light is a normally incident plane wave, we may set it to A; $\dfrac{\mathrm{e}^{\mathrm{i}kr}}{r}$ represents the change of complex amplitude caused by the propagation of the secondary wave from the slit to point P, where $\mathrm{e}^{\mathrm{i}kr}$ represents the phase delay, while the factor $\dfrac{1}{r}$ reflects the change in amplitude due to propagation. Since $r \gg \lambda$, when r varies only by an amount comparable to a wavelength, the amplitude change can be neglected, and thus $\dfrac{1}{r}$ can be considered as some constant $\dfrac{1}{r_1}$ depending on the positions of the light source and the observation point, and can be taken outside the integral; however, the phase change is extremely sensitive to variations in r, where a change of order one wavelength causes a 2π phase shift; $\mathrm{d}\Sigma$ is an infinitesimal area element at the slit. Therefore, the integral becomes

$$\widetilde{U}(P) = \frac{1}{\mathrm{i}\lambda r_1} \iint\limits_{\Sigma_0} A\mathrm{e}^{\mathrm{i}kr}\, \mathrm{d}\Sigma$$

Establishing the Cartesian coordinate system as shown in Fig. 2, we have $\mathrm{d}\Sigma = \mathrm{d}x\ \mathrm{d}y$; writing r in Cartesian form,

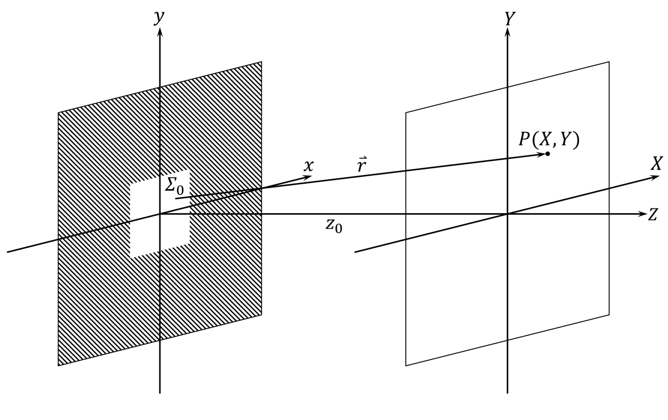

Figure 2: Diffraction of the aperture Σ_0 and the Cartesian coordinate system

$$r = \sqrt{(X-x)^2 + (Y-y)^2 + z_0^2} = z_0 \sqrt{1 + \frac{(X-x)^2}{z_0^2} + \frac{(Y-y)^2}{z_0^2}}$$

Performing a Taylor expansion gives

$$r = z_0 + \frac{(X-x)^2 + (Y-y)^2}{2z_0} - \frac{\left[(X-x)^2 + (Y-y)^2\right]^2}{8z_0^3} + \cdots$$

with the convergence condition $(X-x)^2 + (Y-y)^2 < z_0^2$.

Under the Fresnel approximation, the spherical wavefront of the secondary wave is approximated as a paraboloidal wavefront:

$$r \approx z_0 + \frac{(X-x)^2+(Y-y)^2}{2z_0} = z_0 + \frac{X^2+Y^2}{2z_0} + \frac{x^2+y^2}{2z_0} - \frac{xX+yY}{z_0}$$

Here $\dfrac{k[(X-x)^2+(Y-y)^2]^2}{8z_0^3} \ll \pi$, i.e. $\dfrac{[(X-x)^2+(Y-y)^2]^2}{4\lambda} \ll z_0^3$; under these conditions, $\exp\{\cdots\}$ terms involving higher-order phase contributions can be neglected.

Under the Fraunhofer approximation, the secondary wavefront is approximated as a plane wavefront:

$$r \approx z_0 + \frac{X^2+Y^2}{2z_0} - \frac{xX+yY}{z_0}$$

Here $k(x^2+y^2)/(2z_0) \ll \pi$, i.e. $(x^2+y^2)/\lambda \ll z_0$, equivalently $\rho^2/\lambda \ll z_0$ (far-field condition); under these conditions, $\exp(\mathrm{i}k(x^2+y^2)/(2z_0)+\cdots)$ contributes negligibly to the phase.

We focus on Fraunhofer diffraction. Taking $r_1 = z_0$ and substituting the approximation for r into the integral produces

$$\begin{aligned}
\widetilde{U}[P(X,Y)] &= \frac{\mathrm{e}^{\mathrm{i}kz_0}\cdot \mathrm{e}^{\mathrm{i}k\frac{X^2+Y^2}{2z_0}}}{\mathrm{i}\lambda z_0}\iint\limits_{\Sigma_0} A\mathrm{e}^{-\mathrm{i}k\frac{xX+yY}{z_0}}\,\mathrm{d}x\,\mathrm{d}y \\
&= \widetilde{C}\iint\limits_{\Sigma_0} A\mathrm{e}^{-\mathrm{i}2\pi\left(\frac{X}{\lambda z_0}x+\frac{Y}{\lambda z_0}y\right)}\,\mathrm{d}x\,\mathrm{d}y \\
&= \widetilde{C}\iint\limits_{\Sigma_0} A\mathrm{e}^{-\mathrm{i}2\pi\boldsymbol{f}\cdot\boldsymbol{r_0}}\,\mathrm{d}\boldsymbol{r_0}
\end{aligned}$$

where $\widetilde{C} = \dfrac{\mathrm{e}^{\mathrm{i}kz_0}\cdot \mathrm{e}^{\mathrm{i}k\frac{X^2+Y^2}{2z_0}}}{\mathrm{i}\lambda z_0}$, $\boldsymbol{f} = [X/(\lambda z_0)\quad Y/(\lambda z_0)]^T$, $\boldsymbol{r_0} = [x\quad y]^T$.

According to the Kirchhoff boundary condition, the field on the opaque part of the diffraction screen is zero, so the integration region can be extended from the aperture Σ_0 to the entire diffraction plane Σ, and even to all of $\mathbb{R}^2$. Thus

$$\begin{aligned}
\widetilde{U}[P(X,Y)] &= \widetilde{C}\iint\limits_{\Sigma_0} A\mathrm{e}^{-\mathrm{i}2\pi\boldsymbol{f}\cdot\boldsymbol{r_0}}\,\mathrm{d}\boldsymbol{r_0} \\
&= \widetilde{C}\iint\limits_{-\infty}^{\infty} U_0(\boldsymbol{r_0})\mathrm{e}^{-\mathrm{i}2\pi\boldsymbol{f}\cdot\boldsymbol{r_0}}\,\mathrm{d}\boldsymbol{r_0} \\
&= \widetilde{C}\mathscr{F}[U_0(\boldsymbol{r_0})]
\end{aligned}$$

where

$$U_0(\boldsymbol{r_0}) = \begin{cases} A & (x,y)\in\Sigma_0 \\ 0 & (x,y)\notin\Sigma_0 \end{cases}$$

and $\mathscr{F}[U_0(\boldsymbol{r_0})]$ is its 2D Fourier transform.

On the computer, the Fourier transform can be implemented using the fast Fourier transform (FFT), an efficient algorithm for computing the discrete Fourier transform (DFT). The first step is to discretize the signal. For convenience, we use a matrix to represent the discretized aperture distribution $U_0(\boldsymbol{r_0})$, giving a 200×200 grid. For example, a square aperture can be represented as

$$\mathbf{U_0} = \begin{bmatrix} 0 & \cdots & \cdots & \cdots & \cdots & \cdots & 0 \\ \vdots & 1 & 1 & 1 & 1 & 1 & \vdots \\ \vdots & 1 & 1 & 1 & 1 & 1 & \vdots \\ \vdots & 1 & 1 & 1 & 1 & 1 & \vdots \\ \vdots & 1 & 1 & 1 & 1 & 1 & \vdots \\ \vdots & 1 & 1 & 1 & 1 & 1 & \vdots \\ 0 & \cdots & \cdots & \cdots & \cdots & \cdots & 0 \end{bmatrix}_{200\times 200}$$

Simulation details and code are provided in the Appendix. Here we show several simulated diffraction patterns and their corresponding experimental counterparts in Fig. 3.

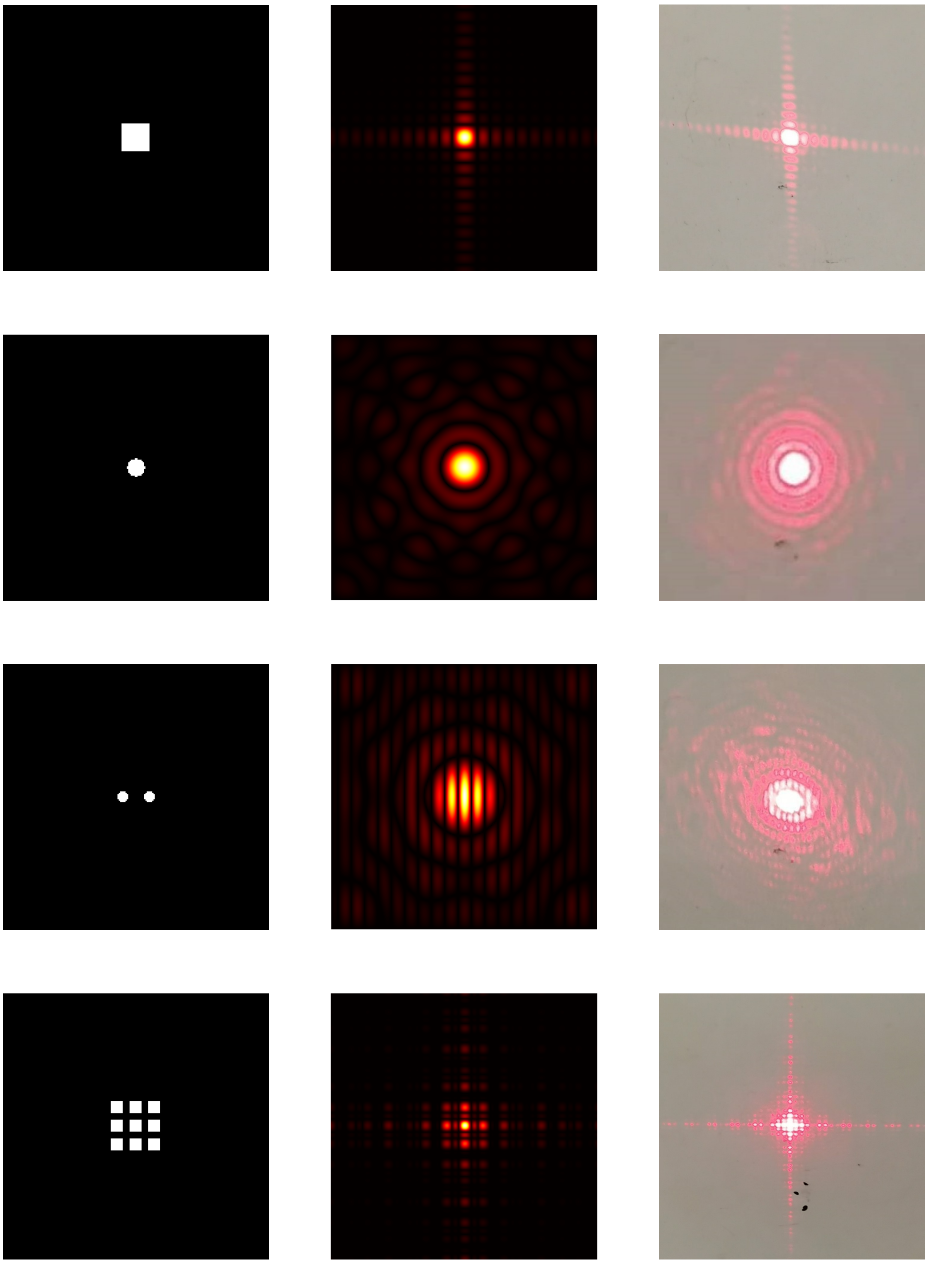

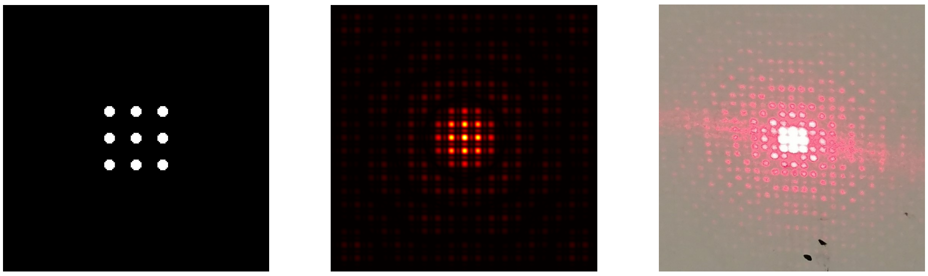

(a) Diffraction screen (b) Simulation (c) Experiment

Figure 3: Comparison of simulated and experimental diffraction patterns

We can see that the simulated diffraction patterns closely resemble the experimental ones, indicating that FFT-based diffraction simulation is highly accurate. Therefore, we can use this method to obtain diffraction patterns for a wide variety of apertures. Additional simulated patterns are provided in the Appendix.

Appendix

1. Specific implementation details of Fraunhofer diffraction simulation and MATLAB code.

```
% This code is adapted from:
% "Physical Optics: Fraunhofer Diffraction"
% by the Multiverse Observer - Zhihu Article
% https://zhuanlan.zhihu.com/p/438807519

clc;
clear;

% Define diffraction plane
N1 = 200;   % grid points
x1 = linspace(-1 , 1 , N1);
y1 = linspace(-1 , 1 , N1);
[X1,Y1] = meshgrid(x1,y1);

% Define observation plane
N = 200;
x = linspace(-10 , 10 , N);
y = linspace(-10 , 10 , N);
[X,Y] = meshgrid(x,y);

U1 = zeros(N1,N1);  % amplitude distribution on diffraction plane

U1(sqrt(X1.^2 + Y1.^2) < 1/15) = 1;  % circular aperture
% Replace the above with other code to generate other aperture shapes

U = zeros(N,N);     % amplitude on observation plane

% FFT-based Fraunhofer diffraction
U(:,:) = fftshift(fft2(U1));    % FFT
U = abs(U);     % magnitude

figure();
surface(U,'edgecolor','none','facecolor','interp');
xlabel('x');
ylabel('y');
colormap hot;
```

```
axis equal;
```

Below we give some explanation. Earlier, we derived:

$$\widetilde{U}[P(X,Y)] = \frac{\mathrm{e}^{\mathrm{i}kz_0} \cdot \mathrm{e}^{\mathrm{i}k\frac{X^2+Y^2}{2z_0}}}{\mathrm{i}\lambda z_0} \mathscr{F}[U_0(\boldsymbol{r_0})]$$

where $U_0(\boldsymbol{r_0})$ is the aperture intensity distribution matrix (represented as `U1`). To obtain the simulated diffraction pattern, we compute the intensity distribution on the observation plane:

$$\left|\widetilde{U}[P(X,Y)]\right| = \left|\frac{\mathrm{e}^{\mathrm{i}kz_0} \cdot \mathrm{e}^{\mathrm{i}k\frac{X^2+Y^2}{2z_0}}}{\mathrm{i}\lambda z_0}\right| \cdot |\mathscr{F}[U_0(\boldsymbol{r_0})]| = \frac{|\mathscr{F}[U_0(\boldsymbol{r_0})]|}{\lambda z_0}$$

Since we are only interested in the relative intensity distribution, not the absolute magnitude, the constant factor $1/(\lambda z_0)$ is ignored, leaving only the Fourier transform term. MATLAB's `fft2()` computes the 2-D FFT, `fftshift()` centers the spectrum, and `abs()` takes the magnitude. Finally, `surface()` visualizes the result. Thus, we obtain a complete Fraunhofer diffraction simulation.

2. Additional simulated diffraction patterns for various apertures. In this section, we first show the generated aperture shapes and then the simulated diffraction patterns. Note especially the relationship between aperture size and the clarity of diffraction patterns.

   (a) Five-pointed star aperture diffraction

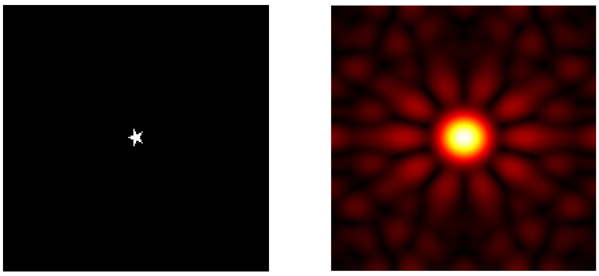

   (b) Circular ring aperture diffraction

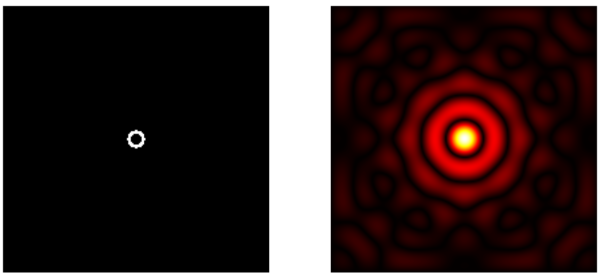

(c) Solid square aperture diffraction

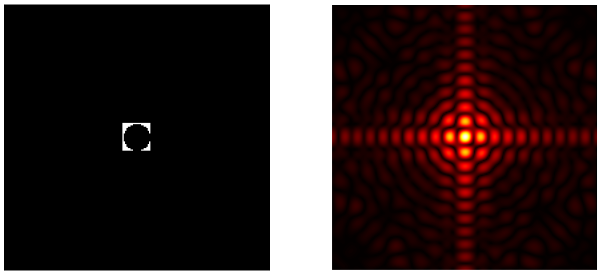

(d) Isosceles triangle aperture diffraction

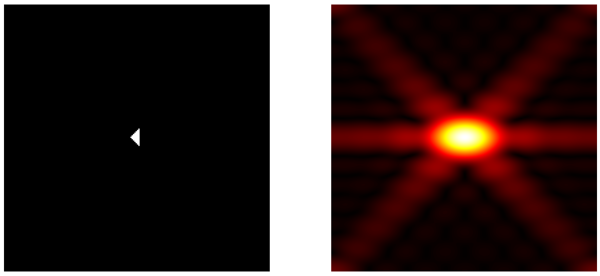

(e) Cross-shaped aperture diffraction

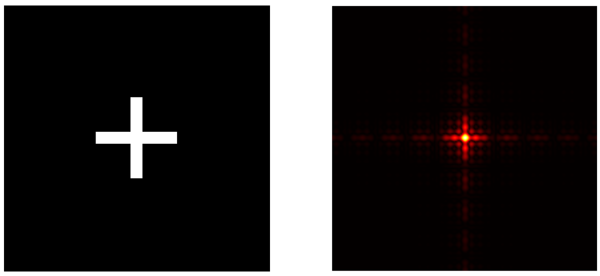

(f) Plum-flower-shaped aperture diffraction

From qualitative observation of these apertures and their corresponding diffraction patterns, we can conclude the following: the larger the aperture size, the less distinct the diffraction pattern becomes, and the weaker the diffraction effects are.